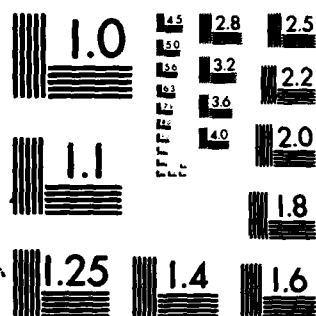


AD-A096 225 COLORADO STATE UNIV FORT COLLINS DEPT OF PHYSICS F/G 20/12  
ELECTRONIC PROPERTIES OF III-V SEMICONDUCTOR INTERFACES.(U)  
NOV 80 J R SITES N00014-76-C-0976  
UNCLASSIFIED SF29 NL



END  
DATE  
FBI  
4-11  
DTIC



MICROCOPY RESOLUTION TEST CHART  
NATIONAL BUREAU OF STANDARDS-1963-A

AD A 096225

**ELECTRONIC PROPERTIES OF III-V SEMICONDUCTOR INTERFACES**

Final Report: November 1980  
ONR Contract N00014-76-C-0976  
Contract Authority NR 243-015

by  
James R. Sites

Report SF 29

Department of Physics  
Colorado State University  
Fort Collins, Colorado 80523

Accession For	
NTIS GRA&I	<input checked="checked" type="checkbox"/>
DTIC TAB	<input type="checkbox"/>
Unannounced	<input type="checkbox"/>
Justification	
Distribution/	
Availability Codes	
Dist	Special and/or
	Special

**A**

Approved for public release; distribution unlimited.  
Reproduction in whole or part is permitted for any  
purpose of the United States Government.

⑨ Final rept.  
Jun 76 - Sep 80

Unclassified

SECURITY CLASSIFICATION OF THIS PAGE (When Data Entered)

REPORT DOCUMENTATION PAGE		READ INSTRUCTIONS BEFORE COMPLETING FORM
1. REPORT NUMBER ⑭ SF 29	2. GOVT ACCESSION NO. AD-A096225	3. RECIPIENT'S CATALOG NUMBER
4. TITLE (and Subtitle) ⑥ Electronic Properties of III-V Semiconductor Interfaces.		5. TYPE OF REPORT & PERIOD COVERED Final (6/76 - 9/80)
6. PERFORMING ORG. REPORT NUMBER		7. CONTRACT OR GRANT NUMBER(s) ⑮ N00014-76-C-0976
8. AUTHOR(s) ⑩ James R. Sites		9. PROGRAM ELEMENT, PROJECT, TASK AREA & WORK UNIT NUMBERS PE 61153 N NR 253-015 RR 021-02-03
9. PERFORMING ORGANIZATION NAME AND ADDRESS Colorado State University Fort Collins, CO 80523		10. REPORT DATE ⑪ 30 November 1980
11. CONTROLLING OFFICE NAME AND ADDRESS Office of Naval Research Electronic and Solid State Sciences Program Arlington, VA 22217		12. NUMBER OF PAGES 27
14. MONITORING AGENCY NAME & ADDRESS (if different from Controlling Office) ⑬ KR02102		15. SECURITY CLASS. (of this report) Unclassified
16. DISTRIBUTION STATEMENT (of this Report) Approved for public release; distribution unlimited. ⑭ KR0210203		18a. DECLASSIFICATION/DOWNGRADING SCHEDULE
17. DISTRIBUTION STATEMENT (of the abstract entered in Block 20, if different from Report)		
18. SUPPLEMENTARY NOTES ONR Scientific Office Telephone: (202) 696-4218		
19. KEY WORDS (Continue on reverse side if necessary and identify by block number) Indium Phosphide      Impurity Band Gallium Arsenide Mobility MESFET JFET		
20. ABSTRACT (Continue on reverse side if necessary and identify by block number) Final contract year dealt with dc transport in InP and GaAs device structures at low temperatures and high magnetic fields. Primary emphasis was on the mobility profile in field effect transistors, with secondary emphasis on basic bulk transport mechanisms. In previous years, studies were made of GaAs MIS structures, encapsulation of GaAs for annealing, and electronic profiling of InAs layers.		

## CONTENTS

1. Introduction .....	1
2. Indium Phosphide Structures .....	2
3. Gallium Arsenide MESFET's .....	6
4. Gallium Arsenide JFET's .....	11
5. Short Channel Devices .....	13
6. Impurity Band Transport .....	15
7. Comments on Final Year .....	20
8. Reports and Publications .....	20

## FIGURES

Fig. 1. Device structures studied.....	3
Fig. 2. Mobility of pseudo-inversion mode InP devices.....	5
Fig. 3. Mobility and conductance of depletion mode InP transistor.....	7
Fig. 4. Temperature dependence of mobility, conductance, and pinch-off voltage for depletion mode InP device.....	8
Fig. 5. Mobility and channel electron density for five GaAs MESFET's....	10
Fig. 6. Influence of magnetic field on transferred electron effect.....	12
Fig. 7. Mobility of enhancement mode GaAs JFET.....	14
Fig. 8. Current and conductance of short channel GaAs current limiter.....	16
Fig. 9. GaAs Hall coefficient showing impurity band transition.....	18
Fig. 10. Magnetic field dependence of GaAs conductivity.....	19

## 1. INTRODUCTION

The four year duration of ONR Contract N00014-76-C-0976 was divided into two somewhat distinct phases. The first three years' work was all performed at Colorado State University. It dealt with (1) metal-insulator-semiconductor (MIS) structures on GaAs, (2) encapsulation of GaAs with oxides and nitrides of silicon and aluminum for annealing purposes, and (3) electronic profiling of thin InAs layers. This work was summarized in the 1979 annual report (Report SF 25, available on request), and will not be repeated except for the list of publications and reports (Sec. 8).

During the final year of this Contract, Prof. Sites worked at the Naval Ocean Systems Center (NOSC) in San Diego; the results and conclusions of that year will be reported in some detail in the following sections. The goal was to expand our knowledge of transport processes in actual device structures. The theme of the measurements performed was dc conductivity and Hall coefficient in high magnetic fields and at low temperatures. Systems studied included (1) indium phosphide field effect transistor structures with silicon devices for reference, (2) gallium arsenide depletion mode Schottky barrier transistors (MESFET), (3) gallium arsenide depletion and enhancement mode junction field effect transistors (JFET), and (4) gallium arsenide epitaxial layers cooled to the impurity band regime.

Much of the transport work was performed in collaboration with Harry Wieder of NOSC. Considerable assistance and advice was also received from the other members of the NOSC staff, particularly Fred Nedoluha, Dave Collins, Larry Meiners, Derek Lile, and Carl Zeisse. And several of the samples studied were supplied by industrial colleagues including Rainer Zuleeg of McDonnell-Douglas, Joe Diesel of Hewlett-Packard, Tom Mills and Ron Kaelberer of TRW, and Ralph Williams of Texas Instruments.

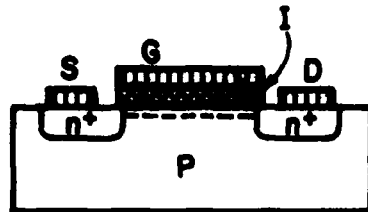
## 2. INDIUM PHOSPHIDE STRUCTURES

Supplementary to the NOSC program for the development of high speed indium phosphide devices, measurements were made of the InP channel transport as a function of gate voltage, temperature, and magnetic field. Most of the structures studied were n-channel pseudo-inversion mode FET's as shown in Fig. 1b. The structure is conceptually similar to the standard inversion mode FET (Fig. 1a) in that a conductive channel is formed by inducing a large curvature in the energy bands near the semiconductor surface. In contrast to the standard structure with a p-type substrate, the pseudo-inversion mode device forms the conductive channel in a semi-insulating substrate. Potential advantages are the lack of capacitive coupling to the substrate and a somewhat lower turn-on voltage.

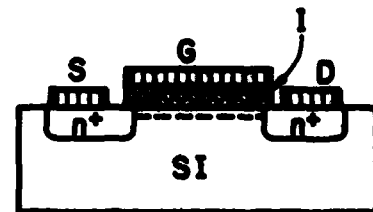
Magnetoresistance was utilized as a tool to deduce the channel carrier mobility, and a comparison was made to field effect mobilities measured under the same conditions. The magnetoresistance technique is particularly powerful because it does not require assumptions about surface states and because the typical FET geometry is a good approximation to the Corbino disk analysis where  $\Delta\rho/\rho = \mu^2 B^2$  for  $\mu B \lesssim 1$ . Field effect mobility, which works well for silicon, suffers in systems with large numbers of surface states because one cannot directly separate gate induced free carriers from induced trapped surface charge. Thus, changes in the channel carrier density may not be simply given by the capacitor charging relation  $\Delta N = \Delta V_G C/qA$ .

The specific InP devices measured had a 1000 Å plasma deposited SiO<sub>2</sub> gate insulator and a gate length of 4 μm. Contacts were made by epitaxial growth of heavily doped n-type InP. Curve tracer displays of the transistor characteristics were qualitatively similar to standard silicon transistors.

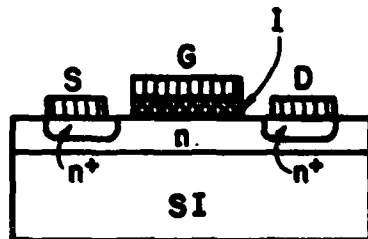




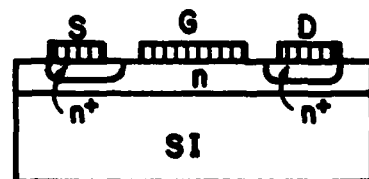
a. Inversion mode FET [Si]



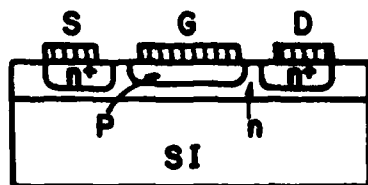
b. Pseudo-inversion mode FET [InP]



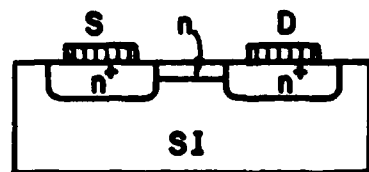
c. Depletion mode insulated gate FET [InP]



d. Depletion mode Schottky barrier FET



e. Depletion or enhancement mode p-n junction gate FET [GaAs]



f. Current limiter [GaAs]

Fig. 1. Device structures studied.

They were, however, not flat in the saturation region, and the transconductance dropped off somewhat (~25%) as dc conditions were approached. The latter is interpreted as an indication that slow trapping processes were present.

The magnetoresistance and field effect mobilities, as a function of gate voltage, are shown in Fig. 2 for several different temperatures. Source-drain voltages were generally 50 or 100 mV where the channel current is approximately linear in voltage. Both magnetoresistance and field effect mobilities are average channel mobilities and not incremental mobilities. Instability in the value of the turn-on voltage made determination of its temperature dependence difficult. It was, however, generally in the 0-1 volt range. The general trend in Fig. 2 is for the mobility of a low density channel to increase with gate voltage and then level off close to  $1000 \text{ cm}^2/\text{V-sec}$ . Gate leakage precluded study of higher channel densities than those shown. There seems, however, to be a gradual fall-off in both mobilities for densities of  $10^{12}$  and above. The two mobilities agree well in magnitude at lower temperatures. Closer to room temperature, the field effect mobility appears to be artificially low, perhaps due to the surface state effect mentioned above. Hall measurements by Larry Meiners on a similar sample show rough agreement with the data of Fig. 2.

A search was made for quantum oscillations in the magneto-conductance of the InP pseudo-inversion layer. An n-channel silicon MOSFET used for reference showed very pronounced oscillations when the gate voltage was varied in a constant magnetic field of 4 tesla or greater. The period of the oscillations was inverse to the magnetic field and the temperature dependence consistent with an effective mass of 0.20 to 0.25. The InP device under the same conditions, however, did not show the quantum

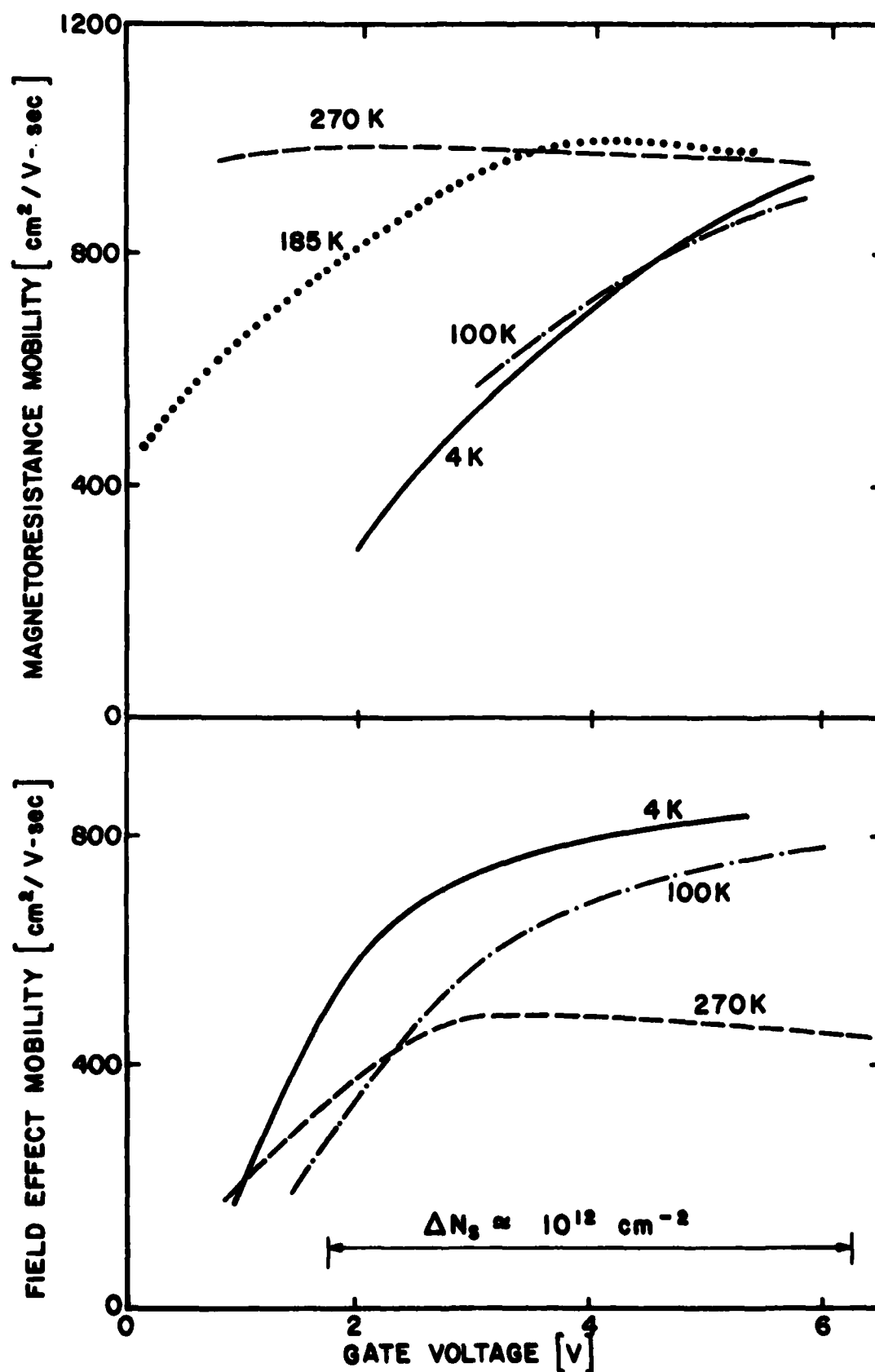


Fig. 2. Mobility of pseudo-inversion mode InP devices.

oscillations. Presumably the explanation is that the somewhat lower mobility ( $\sim 1000 \text{ cm}^2/\text{V-sec}$ ) would require a magnetic field of 10 tesla, just beyond the range of the magnet used. Higher field measurements at Grenoble (K. v. Klitzing, Th. Englert, and D. Fritzsche, J. Appl. Phys., to be published) have subsequently demonstrated the existence of quantum oscillations in similar InP devices.

A second type of InP structure, the depletion mode MIS transistor, was also studied. The active part of this device was an ion implanted n-layer (see Fig. 1c). Mobility of the channel deduced from magnetoresistance is shown in Fig. 3 using circles. Also shown for reference, particularly to show the approach to pinch-off, is the channel conductance. The channel mobility is lower than that characteristic of bulk material. Furthermore (Fig. 4a), it has only a weak temperature dependence, with the broad maximum occurring just below room temperature. These pieces of information suggest a large amount of impurity scattering.

In addition, the magnetoresistance mobility decreases as pinch-off is approached (Fig. 3), in much the same manner as the GaAs devices described in Sec. 4. Note also that the mobility and conductance approximately track with temperature (Fig. 4b), implying the free carrier density is relatively constant down to 4 K. Finally (Fig. 4c), a pinch-off voltage is observed that decreases with lowered temperature. It is not known whether this shift is due to effects within the oxide or at the semiconductor interface.

### 3. GALLIUM ARSENIDE MESFET'S

A comparative study was made of channel mobilities in GaAs Schottley barrier depletion mode transistors (Fig. 1d) acquired from a variety of

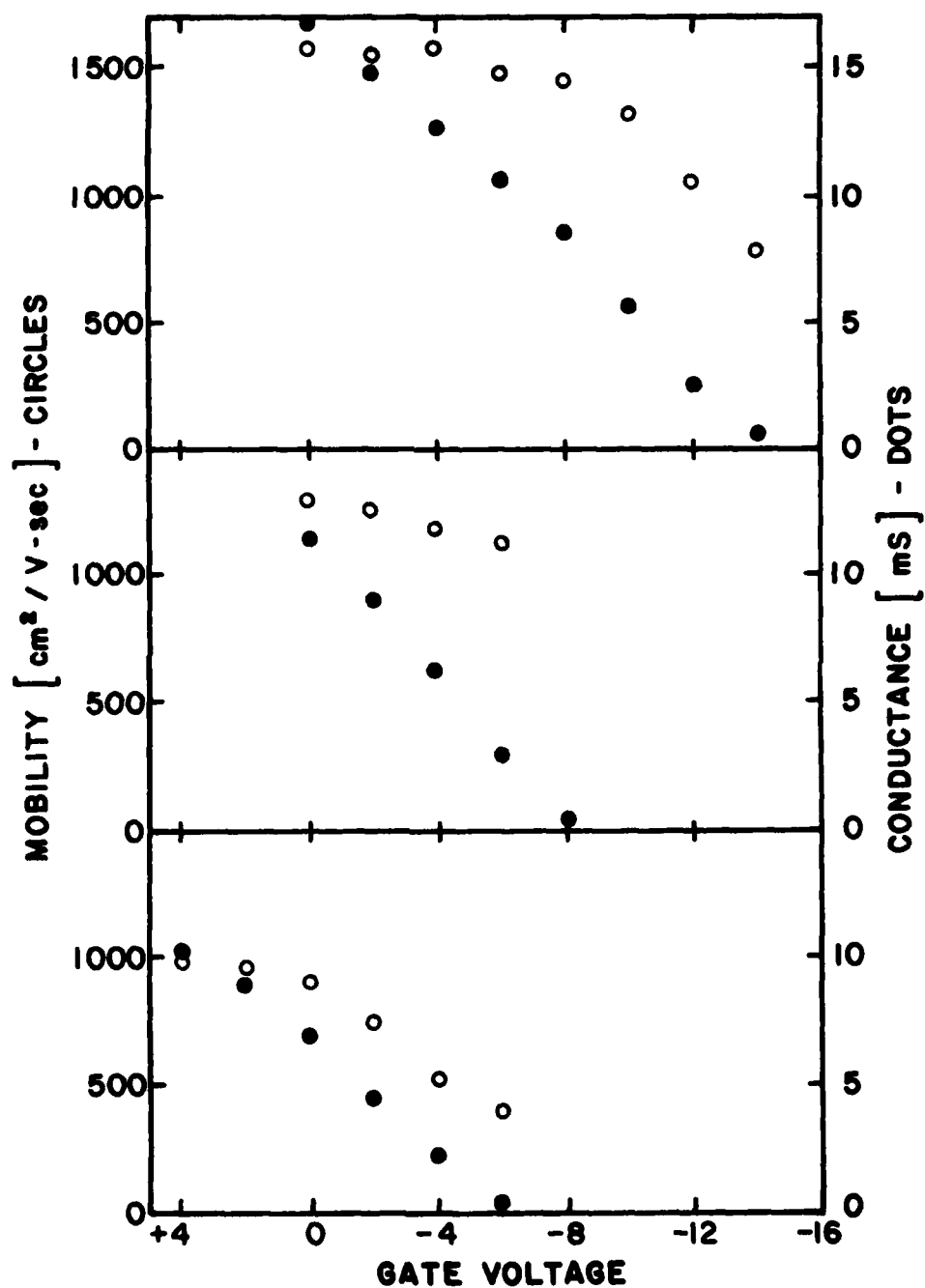


Fig. 3. Mobility and conductance of depletion mode InP transistor. Top 290 K, middle 130 K, bottom 4 K.

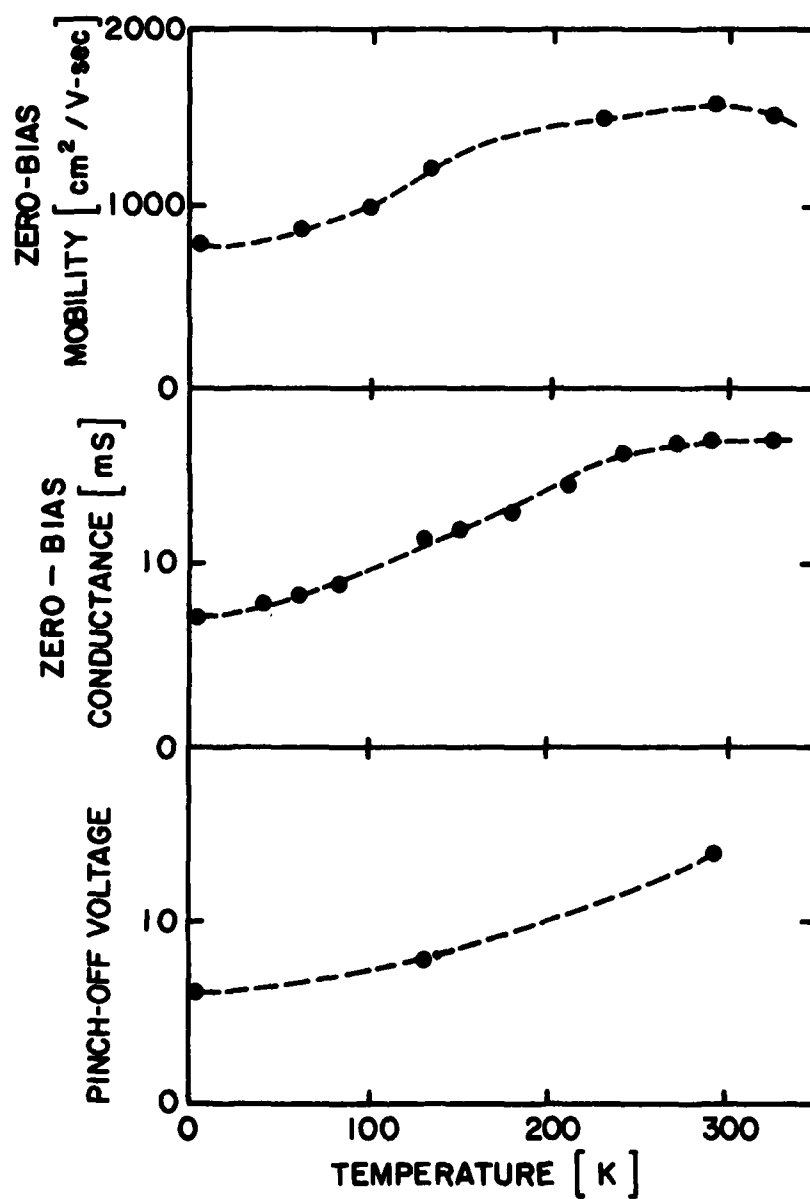


Fig. 4. Temperature dependence of mobility, conductance, and pinch-off voltage for depletion mode InP device.

sources. Details of this study are contained in Report SF 27 which will be published in the December 1980 issue of the IEEE Proceedings on Electron Devices. The MESFET active layers were made by liquid phase epitaxy (LPE), vapor phase epitaxy (VPE), and ion implantation. All devices had an electron concentration the order of  $10^{17}$  and a gate length between 0.6 and 2  $\mu\text{m}$ .

Again the magnetoresistance technique was used to deduce the average channel mobility and its dependence on gate voltage. Source drain voltages were kept at 50 to 100 mV as before. The mobilities for five devices are shown in Fig. 5 with the corresponding values of channel carrier density. The room temperature values were all the order of  $4000 \text{ cm}^2/\text{V-sec}$  and were relatively constant with gate voltage except in the pinch-off region. Near pinch-off, they decreased by 30-60%. The drop in mobility may be due to electron scattering from interfacial defects or to enhanced compensation from chromium diffusion into epilayer. The decrease appears to be somewhat less pronounced in the VPE devices made with buffer layers than in the LPE devices grown directly on the substrate.

The temperature dependence of the MESFET mobilities was fairly weak with the exception of one device (VPE-I) with an apparent composition grading so that part of the channel was in the  $10^{16} \text{ cm}^{-3}$  range. This part of the channel increased in mobility from  $4800 \text{ cm}^2/\text{V-sec}$  at room temperature to  $10,000 \text{ cm}^2/\text{V-sec}$  near 100 K. The pinch-off voltage of the GaAs MESFET's was very steady with temperature (<0.2 volt change) in contrast with the InP device in the previous section.

The effect of magnetic field on transistors operated in the saturation region was also examined. (Report SF 30; to be submitted to IEEE Electron

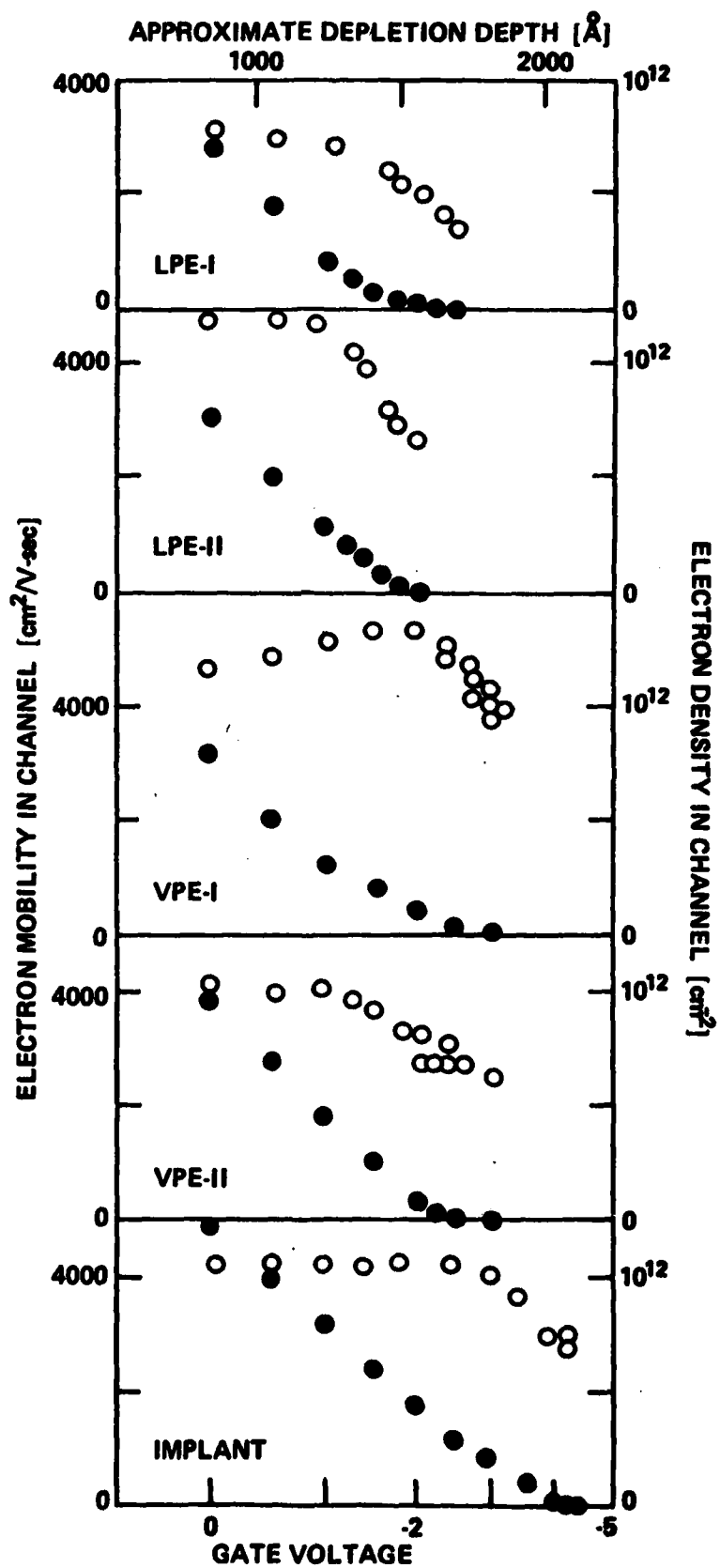


Fig. 5. Mobility and channel electron density for five GaAs MESFET's.



Device Letters.) In general, the short channel devices showed a clear onset of electron transfer as exhibited by a downward kink (See Fig. 6) in the transistor curves at a source-drain voltage corresponding to an electric field near  $10^4$  V/cm. As the magnetic field was increased, the kink became less pronounced (Fig. 6a) and moved to slightly higher voltages (Fig. 6c). It disappeared altogether at fields above 2 tesla. Presumably, the explanation is that when the effective electron mobility in the central valley is sufficiently reduced (in this case to about  $2000 \text{ cm}^2/\text{V-sec}$ ) that the transition to a secondary valley is both more difficult to achieve and has less impact on the transistor operation when it does occur.

#### 4. GALLIUM ARSENIDE JFET'S

Another type of device studied was the GaAs junction field effect transistor (JFET). These devices, shown in Fig. 1e, were made by a double ion implantation technique at McDonnell-Douglas. Conceptually, they are very similar to the MESFET, and some effort was made to compare the two types of structure.

One group of the JFET's studied were fabricated in the standard depletion mode configuration where the p-type gate was implanted into the top part of a thicker n-channel. These devices were normally ON and required a negative gate voltage to turn off. Other devices were implanted in such a way that the n-channel remaining after the p-implant was very thin and fully depleted under zero bias. These enhancement mode devices are normally OFF and require a forward bias across the junction for current flow in the channel. The operating range between channel turn-on and significant forward current through the diode is inherently fairly small.

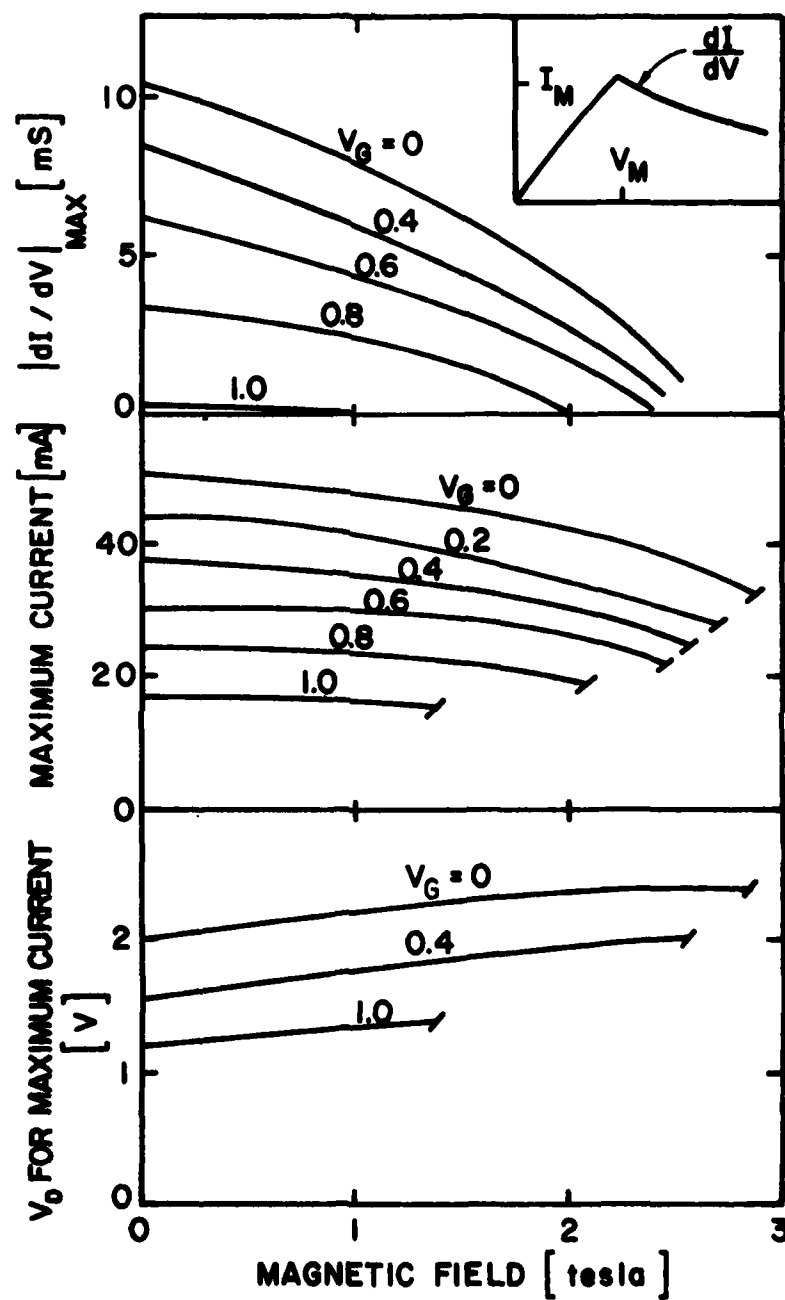


Fig. 6. Influence of magnetic field on transferred electron effect.

Mobilities were once again deduced from magnetoresistance measurements. The depletion mode results were quite similar to the MESFET results in Fig. 5. The mobility magnitude was approximately  $4000 \text{ cm}^2/\text{V-sec}$ , increasing slightly at reduced temperatures and decreasing near pinch-off. A set of results from one of the enhancement mode devices is shown in Fig. 7. Maximum mobility in this case is closer to  $3000 \text{ cm}^2/\text{sec}$ , probably because the thinner channel is inherently close to a pinch-off condition. This reduction may be a reasonable price to pay for a normally OFF transistor. Also shown in Fig. 7 is the shift in built-in potential with temperature, and the corresponding change in turn-on voltage of approximately  $-1 \text{ mV/K}$ .

The quality and stability of the JFET diode, particularly under forward bias conditions, was investigated. The earlier studies with MESFET's showed a tendency for the built-in voltage to shift to higher values ( $\Delta V \sim 50 \text{ to } 150 \text{ mV}$ ) when a forward bias is applied to the gate. In some cases the gate suffered irreversible breakdown with relatively little forward current. The ion implanted JFET's did not exhibit either of these effects. Furthermore, down to about  $100 \text{ K}$  they showed very nearly exponential current-voltage curves with a temperature independent quality factor equal to 2.0.

##### 5. SHORT CHANNEL DEVICES

Another class of ion implanted devices supplied by McDonnell-Douglas was the short channel ( $0.5 \mu\text{m}$ ) GaAs structure shown in Fig. 1f. These gateless channels were designed to be used as current limiters in integrated JFET circuitry. Such structures are known to have a non-ohmic current-voltage relationship at low temperatures, and the  $3/2$  power law observed

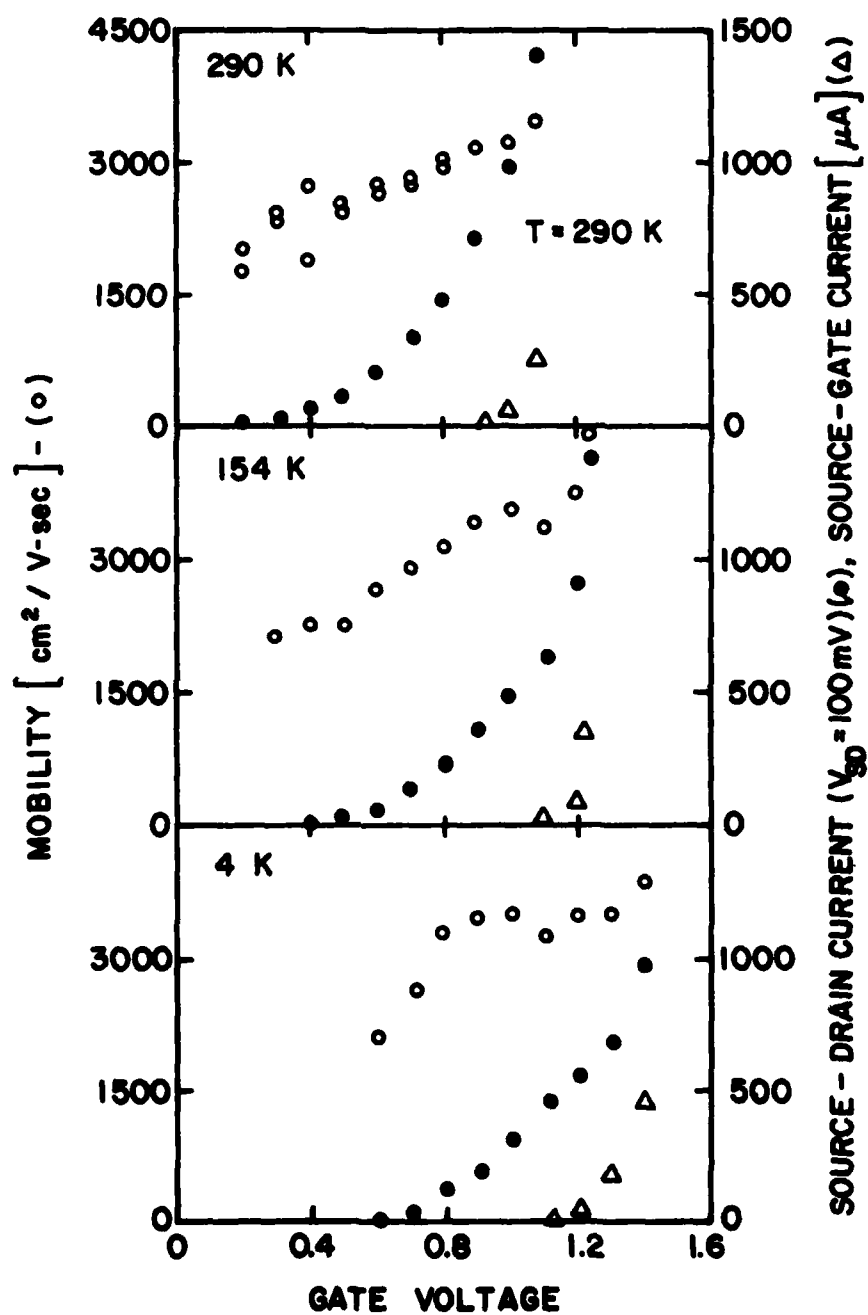


Fig. 7. Mobility of enhanced mode GaAs JFET.

was taken to be suggestive of a ballistic transport process (R. Zuleeg, IEEE Electron Device Lett., EDL-1, 234, 1980).

More exhaustive current-voltage measurements were made with several devices and representative results are shown in Fig. 8. It can be seen that below 200 K the conductance is constant until a critical field (500-5000 V/cm) is reached, and then the current increases more rapidly than voltage. At still higher voltages, current limitation becomes effective and the current approaches a constant value. Magnetoresistance measurements suggest that the channel mobility is too low for ballistic transport from source to drain.

The tentative explanation for Fig. 8 is an increased electron temperature effect. The increase in conductance only occurs at temperatures below the mobility maximum, and the conductance appears to approach the higher temperature values as the effect becomes more pronounced. Furthermore, the increased conductance sets in at electric field values that correspond to an electron drift velocity. Therefore, it is quite possible that the higher velocity electrons in an electric field are simply scattered less than they would be with smaller velocities in zero field.

## 6. IMPURITY BAND TRANSPORT

Details of electronic transport in bulk GaAs and InP in high magnetic fields and low temperatures have been investigated. At temperatures the order of 30 K and below, a significant fraction of the donor impurities are no longer ionized and transport via the conduction band becomes progressively more difficult. If the impurity concentration is sufficiently large, however, that neighboring wave functions overlap, transport is still

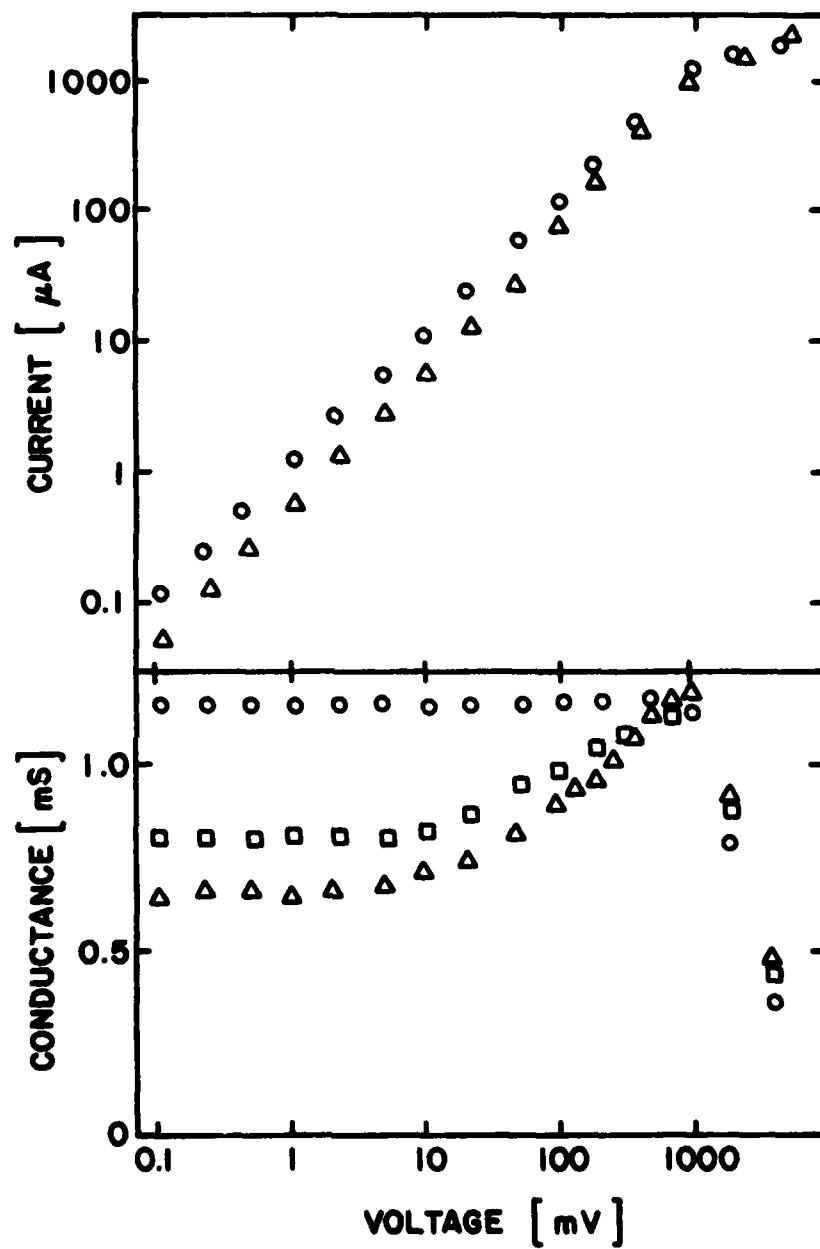


Fig. 8. Current and conductance of short channel GaAs current limiter.

possible. Measurements of dc conductivity and Hall coefficient in this regime have been made, the results analyzed, and a report prepared for publication. (Report SF 28, submitted to Physical Review.)

Historically, impurity band conduction has been studied by comparing samples with different doping concentrations, by varying the carrier concentration in an inversion layer, or, as in the present case, by varying the wavefunction overlap with a magnetic field. We (Dr. A. K. Nedoluha and myself) have interpreted the transport data of bulk samples by assuming there are three conduction possibilities: the conduction band, the upper Hubbard band and the lower Hubbard band. We further assume that the conductivities and the quantity  $B_{\text{HO}}$ , the off-diagonal term in the conductivity tensor, are additive and are of the form  $A_j \exp(-E_j/kT)$ . In fact, the best fit values for  $A_j$  and  $E_j$  for the three bands yield good agreement with the experimental data. In a magnetic field, the coefficients vary systematically and experimental agreement remains good.

Fig. 9 shows the measured Hall coefficient of a  $1.5 \times 10^{16} \text{ cm}^{-3}$  GaAs epilayer function of temperature for several magnetic fields. The pronounced peak occurs at the transition from conduction band transport and that in the upper Hubbard band. The size of the peak should be roughly one-fourth the mobility ratio of the two bands. At high magnetic fields, the wavefunction overlap between neighboring impurities decreases, the effective mobility of the impurity band decreases, and the peak grows, shifting to slightly lower temperature. A second transition between the two Hubbard bands ( $\sim 2 \text{ K}$ ) is much less obvious in the data shown here.

Fig. 10 shows the variation of conductivity with magnetic field as one progressively cools through the same impurity band transition. At high temperatures the transverse magnetoresistance is essentially  $(\mu B)^2$  corrected

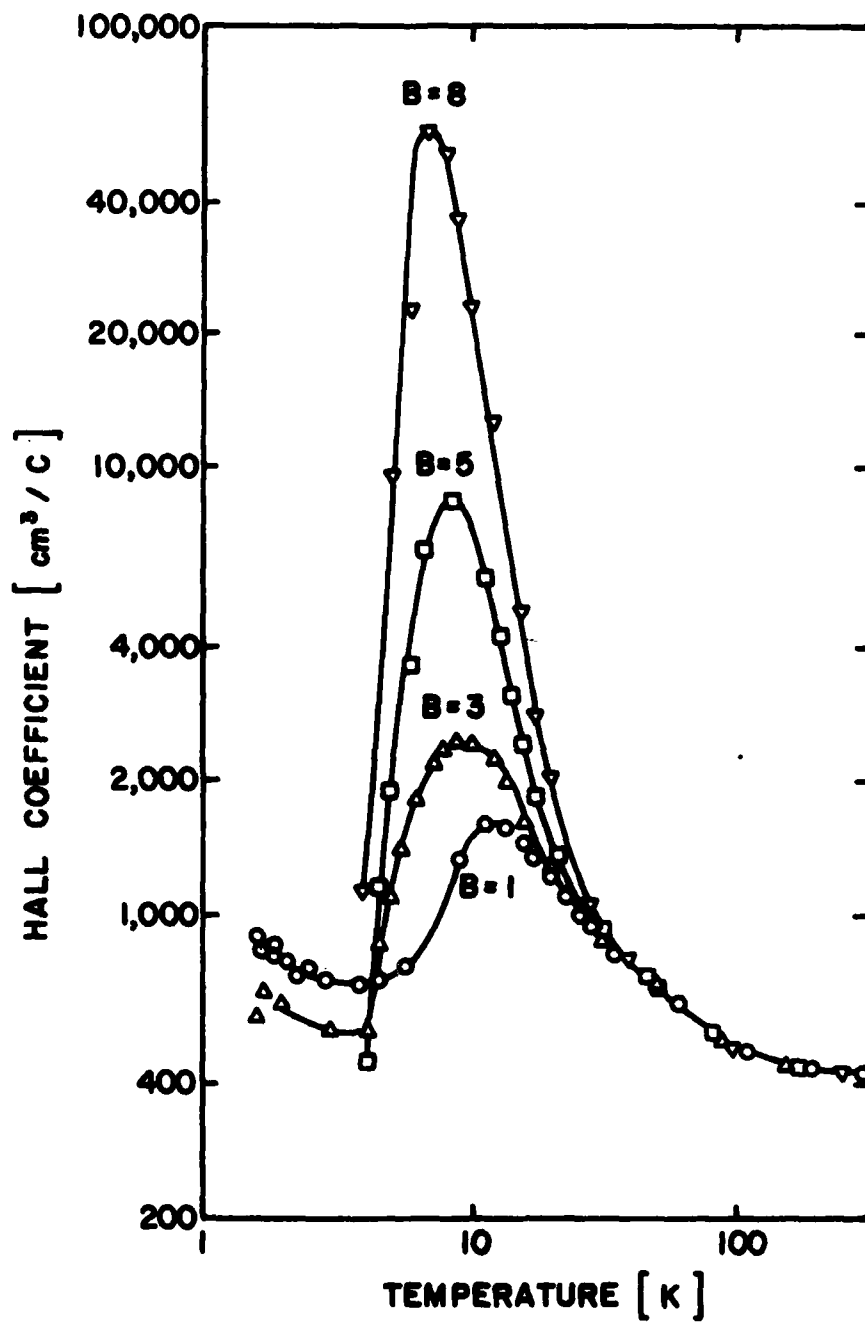


Fig. 9. GaAs Hall coefficient showing impurity band transition.



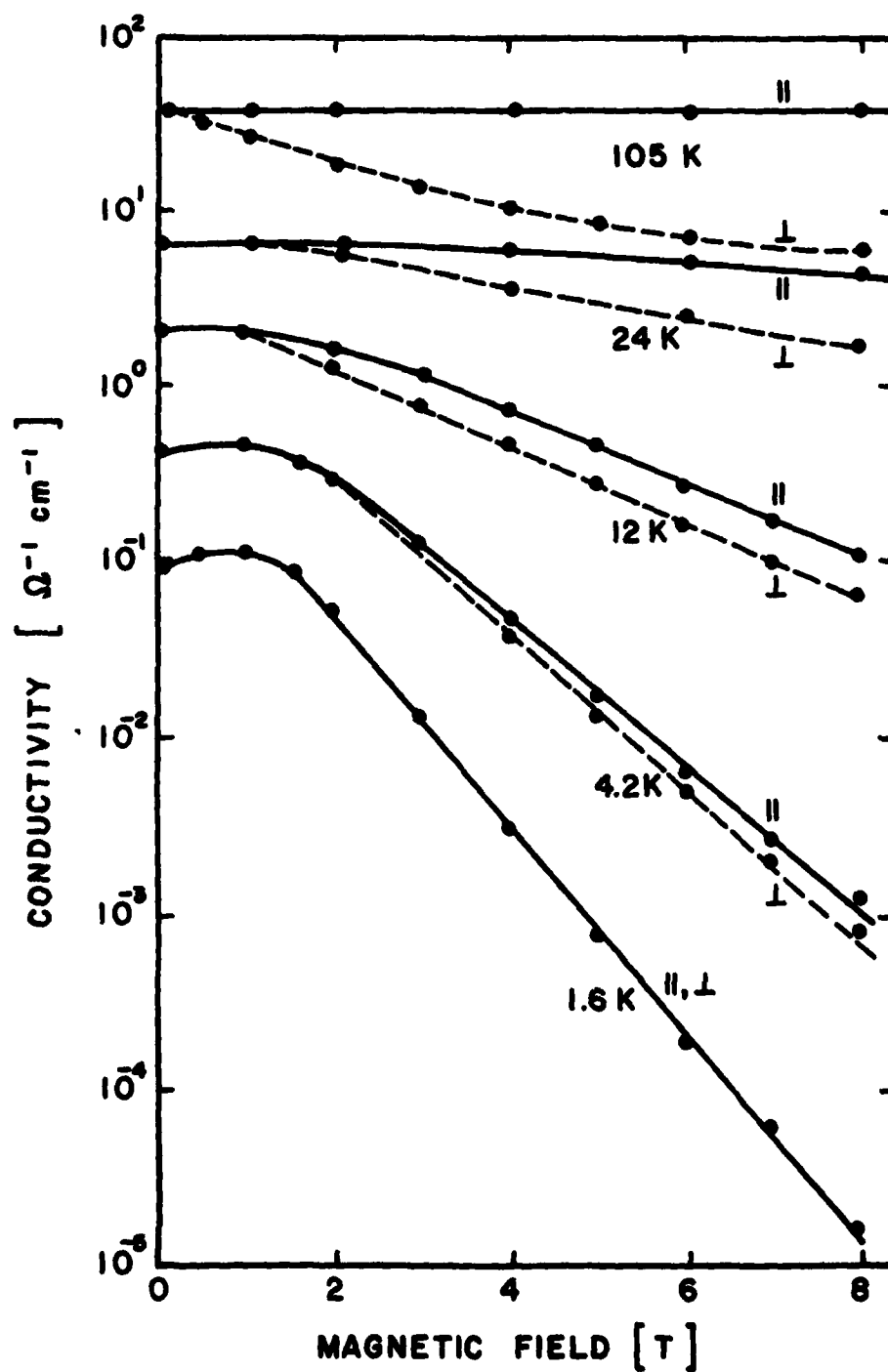


Fig. 10. Magnetic field dependence of GaAs conductivity.

for geometry and the longitudinal magnetoresistance is for practical purposes zero. At lower temperatures, in the impurity band transport regime, the magnetoresistance becomes exponential in the first power of magnetic field, and the distinction between transverse and longitudinal values disappears. There is an onset value for magnetic field effects of two tesla, which roughly corresponds to the field necessary to distort the classical Bohr orbit.

#### 7. COMMENTS ON FINAL YEAR

Overall perspective has been gained on transport processes in compound semiconductors, for the most part using actual device structures. The capabilities of some less common characterization techniques have been explored. The ability to do these measurements in parallel with state-of-the-art development programs, in fact using the same samples, has been particularly rewarding. To me, this past year illustrates the many advantages of cooperation between universities, industry, and government labs. I would encourage increased facilitation of similar opportunities for other scientists.

#### 8. REPORTS AND PUBLICATIONS

The technical reports listed below were generated during the four years Contract N00014-76-C-0976 was in effect. They are available on request. Additionally, the 1979 Annual Report (SF 25) gives a comprehensive summary of the first three years of the Contract.

SF 9: "Oxide Barriers on GaAs by Neutralized Ion Beam Sputtering," by L. G. Meiners, Ru-Pin Pan, and J. R. Sites. J. Vac. Sci. Technol. 14, 961 (1977).

SF 10: "Semiconductor Applications of Thin Films Deposited by Neutralized Ion Beam Sputtering," by J. R. Sites, Thin Solid Films 45, 47 (1977).

SF 11: "Multilayer Model of Indium Arsenide Epilayers," by H. A. Washburn. Thin Solid Films 45, 135 (1977).

SF 13: "Oscillatory Transport Coefficients in InAs Surface Layers," by H. A. Washburn and J. R. Sites, Proc. EP2DS, Berchtesgaden, 1977, and Surf. Sci. 73, 135 (1978).

SF 14: "Silicon Nitride Layers on Gallium Arsenide by Low Energy Ion Beam Sputtering," by L. E. Bradley and J. R. Sites, J. Vac. Sci. Technol. 16, 189 (1979).

SF 15: "Electronic Profile of n-InAs on Semi-insulating GaAs," by H. A. Washburn, J. R. Sites, and H. H. Wieder, J. Appl. Phys. 50, 4872 (1979).

SF 17: "Ion Beam Sputtered  $\text{AlO}_x\text{N}_y$  Encapsulating Films," by Hülya Birey, Sung-Jae Pak, J. R. Sites, and J. F. Wager, J. Vac. Sci. Technol. 16, 2086 (1979).

SF 18: "Cryopumped Ion Beam Sputter Deposition System: Description, Operation, and Optimization," by Sung-Jae Pak, unpublished.

SF 19: "Dielectric-Semiconductor Interfaces of GaAs and InP," by Larry G. Meiners, PhD Thesis, Colorado State Univ., 1979.

SF 20: "Radiative Transitions Induced in Gallium Arsenide by Modest Heat Treatment," by Hülya Birey and James Sites, J. Appl. Phys., 51, 619 (1980).

SF 21: "Thickness and Refractive Index of Thin Transparent Films by Spectrophotometric Transmissivity," by Hülya Birey, unpublished.

SF 22: "Photoluminescence of Gallium Arsenide Encapsulated with Aluminum Nitride and Silicon Nitride," by Hülya Birey, Sung-Jae Pak, and J. R. Sites, Appl. Phys. Lett. 35, 623 (1979).

SF 23: "Depth and Carrier Concentration Dependence of Photoluminescence Features in Heat Treated GaAs:Si," by Hülya Birey and James Sites, unpublished.

SF 24: "Broad Beam Ion Source Operation with Four Common Gases," by S. Pak and J. R. Sites, Rev. Sci. Instrum. 51, 536 (1980).

SF 26: "Sputter Damage in GaAs Exposed to Low Energy Argon Ions," by H. E. Schmidt, P. E. Jensen, and J. R. Sites, unpublished.

SF 27: "Magnetoresistance Mobility Profiling of MESFET Channels," by J. R. Sites and H. H. Wieder, Proc. IEEE ED-27, Dec. 1980.

SF 28: "Impurity Band Transport in Large Magnetic Fields," by J. R. Sites and A. K. Nedoluha, submitted to Phys. Rev.

SF 30: "Magnetic Field Effects on MESFET Characteristics," by J. R. Sites, submitted to IEEE Electron Device Letters.

DISTRIBUTION LIST - FINAL REPORT  
CONTRACT N00014-76-C-0976

1/81

Code 427	4	Dr. H. C. Nathanson	1
Office of Naval Research		Westinghouse Research and	
Arlington, VA 22217		Development Center	
Naval Research Laboratory		Beulah Road	
4555 Overlook Avenue, S. W.		Pittsburgh, PA 15235	
Washington, D. C. 20375		Dr. Daniel Chen	1
Code 6811	1	Rockwell International	
6580	1	Science Center	
Defense Documentation Center	12	P. O. Box 1085	
Building 5, Cameron Station		Thousand Oaks, CA 91360	
Alexandria, VA 22314		Dr. C. Krumm	1
Dr. Y. S. Park	1	Hughes Research Laboratory	
AFWAL/DHR		3011 Malibu Canyon Road	
Building 450		Malibu, CA 90265	
Wright-Patterson AFB		Mr. Lothar Wandinger	1
Ohio, 45433		ECOM/AMSEL/TL/IJ	
ERADCOM	1	Fort Monmouth, NJ 07003	
DELET-M		Dr. Harry Wieder	1
Fort Monmouth, NJ 07703		Naval Ocean Systems Center	
Texas Instruments	1	Code 922	
Central Research Lab		271 Catalina Blvd.	
M.S. 134		San Diego, CA 92152	
13500 North Central Expressway		Dr. William Lindley	1
Dallas, TX 75265		MIT	
Attn: Dr. W. Wisseman		Lincoln Laboratory	
Dr. R. M. Malbon/M.S. 1C	1	F124 A, P. O. Box 73	
Avantek, Inc.		Lexington, MA 02173	
3175 Bowers Avenue		Commander	1
Santa Clara, CA 94304		U. S. Army Electronics Command	
Mr. R. Bierig	1	V. Gelnovatch	
Raytheon Company		(DRSEL-TL-IC)	
28 Seyon Street		Fort Monmouth, NJ 07703	
Waltham, MA 02154		RCA	1
Dr. R. Bell, K-101	1	Microwave Technology Center	
Varian Associates, Inc.		Dr. F. Sterzer	
611 Hansen Way		Princeton, NJ 08540	
Palo Alto, CA 94304			

Enclosure

Hewlett-Packard Corporation Dr. Robert Archer 1501 Page Road Palo Alto, CA 94306	1	D. Claxton MS/1414 TRW Systems One Space Park Redondo Beach, CA 90278	1
Watkins-Johnson Company E. J. Crescenzi, Jr./ K. Niclas 3333 Hillview Avenue Stanford Industrial Park Palo Alto, CA 94304	1	Professor L. Eastman Phillips Hall Cornell University Ithaca, NY 14853	1
Commandant Marine Corps Scientific Advisor (Code AX) Washington, D. C. 20380	1	AIL TECH 612 N. Mary Avenue Sunnyvale, CA 94086 Attn: G. D. Vendelin	1
Communications Transistor Corp. Dr. W. Weisenberger 301 Industrial Way San Carlos, CA 94070	1	Professor Hauser and Littlejohn Department of Electrical Engr. North Carolina State University Raleigh, NC 27607	1
Microwave Associates Northwest Industrial Park Drs. F. A. Brand/J. Saloom Burlington, MA 01803	1	Professor J. Beyer Department of Electrical & Computer Eng. University of Wisconsin Madison, WI 53706	1
Commander, AFAL AFWAL/AADM Dr. Don Rees Wright-Patterson AFB, Ohio 45433	1	Professor Rosenbaum & Wolfe Semiconductor Research Laboratory Washington University St. Louis, MO 63130	1
Professor Walter Ku Phillips Hall Cornell University Ithaca, NY 14853	1	W. H. Perkins Electronics Lab 3-115/B4 General Electric Company P. O. Box 4840 Syracuse, NY 13221	1
Commander Harry Diamond Laboratories Mr. Horst W. A. Gerlach 2800 Powder Mill Road Adelphia, MD 20783	1		
Advisory Group on Electron Devices 201 Varick Street, 9th floor New York, NY 10014	1		

